Expression and protein-binding studies of the *EEN* gene family, new interacting partners for dynamin, synaptojanin and huntingtin proteins

Chi Wai SO*[1], Mai Har SHAM†, Sze Lun CHEW*, Ngai CHEUNG*, Cary K. C. SO*, Sookja K. CHUNG‡, Carlos CALDAS§, Leanne M. WIEDEMANN‖ and Li Chong CHAN*

*Department of Pathology, The University of Hong Kong, Hong Kong, Peoples' Republic of China, †Department of Biochemistry, The University of Hong Kong, Hong Kong, People's Republic of China, ‡Institute of Molecular Biology, The University of Hong Kong, Hong Kong, Peoples' Republic of China, §Department of Oncology, University of Cambridge, Cambridge CB2 2QQ, U.K., and ‖Leukaemia Research Fund Centre, Chester Beatty Laboratories, London SW3 6JB, U.K.

EEN, identified initially as a fusion partner to the mixed-lineage leukaemia gene in human leukaemia, and its related members, *EEN-B1* and *EEN-B2*, have recently been shown to interact with two endocytic molecules, dynamin and synaptojanin, as well as with the huntingtin protein. In the present study, we show that the expression of the *EEN* gene-family members is differentially regulated. Multiple-spliced variants were identified for *EEN-B2*. In the brain, EEN-B1 and EEN-B2 mRNA are preferentially expressed in the cerebellar Purkinje and granule cells, dentate gyrus cells, hippocampal pyramidal neurons and cerebral granule cells. The expression patterns of EEN-B1 and EEN-B2 mRNA in the brain overlap with those of dynamin-I/III, synaptojanin-I and huntingtin, whereas the ubiquitous expression of *EEN* is consistent with that of dynamin-II. In testes, members of the *EEN* family are co-expressed with testis-type dynamin and huntingtin in Sertoli cells and germ cells respectively. Our results on the overlapping expression patterns are consistent with the proposed interaction of *EEN* family members with dynamin, synaptojanin and huntingtin protein *in vivo*. Although all three *EEN* family members bind to dynamin and synaptojanin, *EEN-B1* has the highest affinity for binding, followed by *EEN* and *EEN-B2*. We also demonstrate that amphiphysin, a major synaptojanin-binding protein in brain, can compete with the *EEN* family for binding to synaptojanin and dynamin. We propose that recruitment of the *EEN* family by dynamin/synaptojanin to clathrin-coated pits can be regulated by amphiphysin.

Key words: endocytosis, endophilin family, SH3 domain.

INTRODUCTION

The EEN family [also called the endophilin/Src homology region 3 (SH3)p/SH3GL family] is a new family of SH3-domain-containing proteins that has recently been found to be involved in both normal and malignant cellular processes, including clathrin-mediated endocytosis [1,2] and chromosomal translocation in human leukaemia [3]. The *EEN* gene family consists of at least three members, *EEN*, *EEN-B*1 and *EEN-B*2, which are evolutionarily conserved and show over 70% sequence identity at the amino acid level [3–5]. Proteins of the EEN family can interact with the proline-rich domains (PRDs) of dynamin and synaptojanin via their SH3 domains [2]. These EEN proteins are also co-localized with dynamin, synaptojanin and amphiphysin in the nerve termini of rat brain, where dynamin and synaptojanin can be co-precipitated by antibodies raised against EEN family members [2].

Dynamin is a GTPase involved in synaptic vesicle recycling. It shares similarity to the product of the *Drosophila shibire* gene [6,7], and a temperature-sensitive mutation in the *shibire* gene impairs the endocytosis of synaptic vesicle membrane following exocytosis, disrupting the release of neurotransmitter [8,9]. The functional importance of dynamin in endocytosis has been illustrated further by the conformational change of the dynamin rings formed at the necks of invaginated coated pits that correlate with GTP hydrolysis, which represents a key step leading to vesicle fission from the plasmalemma [10,11]. Synaptojanin is a type II inositol 5-phosphatase containing an N-terminal SacI domain that is homologous with the cytosolic domain of the yeast SacI protein [12]. Inositol phosphate metabolism and yeast SacI protein have been implicated in a variety of membrane-trafficking events, including endocytosis [13]. The role of SacI protein in endocytosis has been supported by the findings that it can mediate ATP transport into the yeast endoplasmic reticulum [14], and a yeast mutant lacking synaptojanin-like genes (*SJL1-L3*) exhibits a severe defect in receptor-mediated and fluid-phase endocytosis [15].

Both dynamin and synaptojanin bind to the SH3 domain of amphiphysin isoforms I and II [16], proteins that were first identified in chicken synaptic fractions [17] and are concentrated in mammalian nerve termini [18]. Amphiphysin also interacts with AP2, an adaptor protein for the plasma-membrane clathrin coat [18,19]. Mutation of the yeast homologues of amphiphysin, RVS 161 and RVS 167, results in an endocytosis defect characterized, in part, by an impairment in α-factor receptor internalization [20]. The disruption of SH3 domain interaction of amphiphysin I in living nerve-termini preparations leads to incomplete synaptic-vesicle endocytosis at the stage of invaginated clathrin-coated pits [21,22], highlighting the role of SH3-domain-mediated interactions in endocytosis. Notably, the EEN family of proteins, apart from amphiphysin, are the only interacting partners containing an SH3 domain enriched in

Abbreviations used: SH3, Src homology region 3; PRD, proline-rich domain; HD, huntingtin; poly(A)$^+$, polyadenylated; ISH, *in situ* hybridization; dpc, days post-coitum; GST, glutathione transferase; RT, reverse transcriptase; CNS, central nervous system; SLMV, synaptic-like microvesicle; LPAAT, lysophosphatidic acid acyltransferase.

[1] To whom correspondence and offprint requests should be addressed, at the present address: Department of Pathology, Stanford University Medical Center, Stanford, CA 94305, U.S.A. (e-mail cwso@stanford.edu).

The nucleotide sequence data reported in this paper have been submitted to the GenBank® and Human Gene Nomenclature Committee, with accession numbers for *EEN-B1* and *EEN-B2*-L1, -L2, -L3 and -L4 of AF036268, AF036269, AF036270, AF036271 and AF036272 respectively.

presynaptic termini [2,23,24]. The physiological significance of the EEN family in endocytosis has been strengthened further by the finding that endophilin I (the rat homologue of EEN-B1), instead of amphiphysin, is the major synaptojanin-binding protein in the rat brain [1].

There is emerging evidence showing that the EEN family may also be involved in the pathogenesis of Huntington's disease [25,26]. Huntingtin (HD) protein, like EEN family members, is concentrated in the presynaptic termini, and enriched in the synaptosomal membrane fractions, together with synaptophysin, dynamin and p145, the latter of which is probably the short isoform of synaptojanin [27]. A recent yeast two-hybrid study has shown that a EEN family member interacts and co-localizes with HD protein in Huntington's disease patients [25]. SH3GL3/EEN-B2 can specifically interact with the Huntington's Disease exon 1 protein (HDex1p), which contains a glutamine repeat in the pathological range. This interaction promotes the formation of insoluble polyglutamine-containing aggregates *in vivo*, and is induced by the length of polyglutamine sequence in HDex1p. The strong and specific binding of EEN-B2 to the HD fragment with an elongated polyglutamine repeat has been suggested to promote the formation of fibrillar structures in neurons, leading to a selective neuronal degeneration in distinct regions (including the cortex and striatum) of the brain of Huntington's disease patients [25].

It has also been shown that the expression and regulation of endocytic molecules that are known at present, including dynamin, synaptojanin and amphiphysin, are very complex [16,23,28–30]. Multiple-splice-variant transcripts are differentially expressed in various tissues, and some splice variants of dynamin have different subcellular localization patterns and functions [31]. However, little is known about the expression and regulation of the EEN family and their interactions with other endocytic molecules. In the present study, we identified three novel splice variants of the *EEN-B2* gene that are differentially expressed in various tissues. We also characterized the expression domains of EEN family members in various human and mouse tissues at different developmental and adult stages, and their binding properties to dynamin and synaptojanin. Our results clearly demonstrate that the expression patterns of the EEN family in the nervous tissue overlap with those of dynamin, synaptojanin and HD, and support their interaction *in vivo*.

EXPERIMENTAL

Library screening and DNA sequencing

EEN cDNA and human expression tag (EST) clones (H50251, H20385 and H19489) encoding EEN-related sequences were labelled with ^{32}P to screen a human fetal-brain cDNA library under low-stringency hybridization and washing conditions [32]. Positive clones were isolated and converted into pBluescript phagemids for restriction mapping and DNA sequencing. All sequencing was performed using fluorescently labelled dideoxy terminators on a 377 Applied Biosystems automated sequencer. The DNA sequence was assembled and analysed, and both the nucleotide and predicted open reading frames were compared with public databases using various online and network facilities.

Amplification of EEN-B1 and EEN-B2 from brain RNA and genomic DNA

Total RNAs were extracted from normal human adult brain, 10-week fetal brain and brain medulloblastoma, and subjected to reverse transcription with random hexamers. Except for EEN-B2-L1 and EEN-B2-L2, which were amplified using the same set of primers [*EEN-B2*(1f) and *EEN-B2*(2r)], specific primers were designed for PCR amplification on random-primed cDNA for the following transcripts, as shown in Table 1; see also Figure 1. EEN-B2-L1 and EEN-B2-L2 transcripts, which differed from each other by a 7-bp deletion in EEN-B2-L2, were distinguished by their different mobility on gel electrophoresis, and confirmed by DNA sequencing. RNA quality was assessed by comparative actin PCR using actin-specific primers. Each actin PCR consisted of 62.5 fg of internal-template control, which would produce a fragment of size approx. 400 bp that was 100 bp larger than the band amplified from human actin cDNA (see Figures 3a and 3c).

Table 1 PCR primers used for amplification of *EEN-B1* and *EEN-B2* variant transcripts

Primer used	Sequences (5′ → 3′)	Purposes
EEN-B1(1f)	gtgatggaaataatgactaa	Amplification of EEN-B1 transcript
EEN-B1(1r)	tttgacctccgacagttc	
EEN-B2(1f)	gctgaagaagcagttccaca	Amplification of EEN-B2-L1 and EEN-B2-L2 transcripts
EEN-B2(2r)	agagagtctttcacctcagc	
EEN-B2(6f)	tcagaagatgaatgaatgg	Amplification of EEN-B2-L3 transcript
EEN-B2(4r)	gaagatattcagtggttt	
EEN-B2(4f)	cagttggctgtgttcataga	Amplification of EEN-B2-L4 transcript: [first round, *B2*(4f) and *B2*(5r); nested, *B2*(5f) and *B2*(5r)]
EEN-B2(5f)	ctgtcgtggtctctatgac	
EEN-B2(5r)	gatgctaaacaccattattc	
EEN-B2(3f)	gaatgctgaacactgtgtcg	Amplification of all EEN-B2-L1–L4 transcripts (ALL-EEN-B2)
EEN-B2(1r)	atcttgtagtaactgaagt	
EEN-B2(2f)	gatgttaccaataaagttgttgcag	Amplification of genomic EEN-B2
EEN-B2(3r)	ccagcaagccttccgtctg	
Actin-1f	actcttccagccttccttcc	Actin PCR
Actin-1r	cgtcatactcctgcttgctg	

A genomic fragment of *EEN-B2* flanking the 7-bp deletion found in *EEN-B2*-L2 was amplified by *EEN-B2*(2f) and *EEN-B2*(4r) from human genomic DNA. The amplified fragment was cloned into pGEM-T vector, and partially sequenced from both ends.

Gene expression studies by Northern blot hybridization and PCR analysis

Polyadenylated [poly(A)$^+$]-selected human and mouse RNA multiple-tissue Northern blots (Clontech, Palo Alto, CA, U.S.A.) were hybridized with a cDNA probe derived from specific coding sequence or the 3′-untranslated regions of the genes. Probes used for hybridization included: (i) a 1.6-kb *Pst*I fragment spanning part of the coding and 3′-untranslated region of *EEN*; (ii) a 2.8-kb probe covering the coding and part of the 3′-untranslated region of *EEN-B1*; and (iii) a 400-bp *EEN-B2* probe derived from the 3′-untranslated region shared by *EEN-B2*-L1, *EEN-B2*-L2 and *EEN-B2*-L3. The probes used for mouse blots were essentially the same as those used for *in situ* hybridization (ISH; see below). Hybridization was performed under standard high-stringency conditions [32]. The expression of EEN-B1 and each of the EEN-B2 transcripts was examined by PCR on a human multiple-tissue cDNA panel (Clontech). In each PCR reaction, approx. 0.4 ng of cDNA from different tissues, previously normalized with six different housekeeping genes, was amplified using 2.5 pmol of gene-specific primers. These primers were

similar to those used for the amplification of EEN-B1 and EEN-B2 transcripts from brain tissues, with one exception, i.e. amplification of total EEN-B2 transcripts (ALL EEN-B2), in which primers *EEN-B2*(3f) and *EEN-B2*(1r) were designed from the common sequence shared by all four EEN-B2 transcripts (Table 1; also see Figure 1). The qualities and normalization of the cDNA panel were assessed by comparison with actin PCR.

ISH

The same murine cDNA templates (kindly given by B. Kay, University of Wisconsin–Madison, Madison, WI, U.S.A.) were used for both whole-mount and section ISH. Riboprobes used for ISH included: (i) a 2-kb fragment covering the coding sequence and both 5′- and 3′-untranslated regions of SH3p8/endophilin II (murine *EEN*); (ii) an 800-bp fragment spanning part of the coding sequence and 5′-untranslated region of SH3p4/endophilin I (murine *EEN-B1*); and (iii) a 900-bp probe covering part of the coding sequence and 3′-untranslated region of SH3p13/endophilin III (murine *EEN-B2*). Whole mount embryo ISH was performed as described previously [33] using digoxigenin-labelled UTP as a substrate for the transcription of probes *in vitro*. Embryos at 8.5- and 9.5-days post-coitum (dpc) were collected from FBB mice and fixed in 4% (v/v) paraformaldehyde overnight before protease K treatment. After overnight hybridization at 65 °C, the embryos were washed three times at 65 °C with 0.2 × SSC (where 1 × SSC is 0.15 M NaCl/0.015 M sodium citrate) for 30 min each. Hybridization signals were detected by ELISA using anti-digoxigenin alkaline phosphatase and X-phosphate/Nitro Blue Tetrazolium. Section ISH was performed using ^{35}S-radiolabelled riboprobes, according to a standard protocol. Mouse embryos or tissues were snap-frozen in liquid nitrogen and then fixed in 4% (v/v) paraformaldehyde for 20 min. Overnight hybridization was performed at 55 °C with a probe concentration of 1×10^8 c.p.m./ml. Non-specific probe binding was washed off at 55 °C with 2 × and 0.2 × SSC for 60 min each. The slides were dipped into emulsion (Amersham Pharmacia Biotech., Little Chalfont, Bucks., England) and exposed for 2–4 weeks before signal development. The sections were counter-stained with haematoxylin and eosin, and silver granules were examined under both a light microscope (Axiophot; Zeiss, Cologne, Germany) and a stereomicroscope (SV11; Zeiss).

Production of glutathione S-transferase (GST) fusion protein and *in vitro*-synthesized proteins

SH3 domains of EEN family members (EEN, EEN-B1 and EEN-B2), human amphiphysin I (Genbank® accession no. U07616; 590–695 amino acids), amphiphysin II (GenBank® accession no. U87558; 496–593 amino acids), and RasGAP (GenBank® accession no. M23379; 274–347 amino acids) were amplified by PCR on appropriate cDNA templates, and cloned in-frame into pGEX vectors that express recombinant GST fusion proteins. Constructs were verified by DNA sequencing prior to the expression of the GST fusion protein in the host strain DH5α upon isopropyl β-D-thiogalactoside induction using a standard method. Various deletion constructs of EEN-B2 were also amplified and cloned into pGEM-T vectors for protein synthesis *in vitro*. Human dynamin-I and the rat synaptojanin 145-kDa isoform were kindly given by De Camilli (Yale University, New Haven, CT, U.S.A.). Following column purification (Qiagen, Hilden, Germany), 1 μg of each plasmid DNA was expressed using the TNT-coupled reticulocyte lysate system (Promega, Madison, WI, U.S.A.) according to the manufacturer's instructions. All protein products were analysed on an SDS/12% (w/v) polyacrylamide gel, and subjected to autoradiography or immunoblotting using an anti-GST antibody.

Competitive GST binding assays

GST fusion proteins (1 μg) were preincubated with glutathionine–Sepharose beads (Amersham Pharmacia Biotech) in NETN buffer [0.5% (v/v) Nonidet P-40/20 mM Tris/HCl (pH 8.0)/100 mM NaCl/1 mM EDTA] for 60 min at 4 °C, and subsequently used for protein competitive-binding assay: ^{35}S-labelled *in vitro*-synthesized dynamin/synaptojanin was added with 1, 5, 25 or 50 μg of competitor proteins to the beads. These proteins were synthesized as GST fusion proteins, except that the GST portions of the fusion proteins had been removed by factor Xa (Amersham Pharmacia Biotech) digestion according to the manufacturer's instructions, so they could not bind to the glutathionine–Sepharose bead. After a 90-min incubation at 4 °C, the beads were washed five times in buffer H [20 mM Hepes (pH 7.7)/50 mM KCl/20% (v/v) glycerol/0.1% (v/v) Nonidet P40/0.007% 2-mercaptoethanol]. Bound proteins were eluted by boiling in SDS/PAGE loading buffer, resolved by electrophoresis and detected by autoradiography. All competitive binding assays were repeated at least twice to confirm the results.

RESULTS

Cloning of the *EEN* gene family

Using *EEN*-related sequences to screen a human fetal-brain cDNA library, several overlapping clones containing *EEN* homologous sequence were identified. Sequence analysis indicated that these clones could be aligned to form five major contigs. Four of these (subsequently referred to as *EEN-B2*-L1 to *EE2-B2*-L4) appeared to be derived from a single gene (*EEN-B2*) and the fifth was referred to as *EEN-B1*, on account of their preferential expression in brain (described below). The three members of the EEN protein family, EEN, EEN-B1 and EEN-B2, share over 70% amino acid sequence identity and highly homologous C-terminal SH3 domains (with 80% amino acid identity). These have also been identified by degenerative PCR amplification, and named as SH3GL1, SH3GL2 and SH3GL3 respectively [5]. BLAST homology searches revealed that EEN, EEN-B1 and EEN-B2 are the human homologues of the mouse endophilin II, endophilin I and endophilin III [4]. The identity between each of the human and mouse homologues is over 85% at the nucleic acid level, and 90% at the amino acid level.

Identification of variant transcripts of EEN-B2

During the course of cDNA library screening, four highly related cDNA clones encoding *EEN-B2* were identified. Sequence analysis and restriction mapping revealed that they represent four different types of EEN-B2 transcripts, i.e. EEN-B2-L1, -L2, -L3 and -L4 (Figure 1). These transcripts could arise from the utilization of alternative transcriptional start sites and splicing variations. Compared with other transcription variants of EEN-B2, EEN-B2-L1 equivalent to EEN-B2 in Figure 1 shows highest overall sequence homology with transcripts of EEN and EEN-B1. Conceptual translation of the EEN-B2-L1 cDNA sequence revealed that the longest open reading frame codes for a 40-kDa polypeptide containing an SH3 domain at the C-terminus and several in-frame, internal methionine codons ($AUG^{I–IV}$ in Figure 1). EEN-B2-L2 is similar to EEN-B2-L1, apart from a 7-bp deletion upstream of AUG^{II}, which could result in a frame-shifted translated protein product. (This -L2 transcript was also represented by the EST clones with accession numbers H50251, H20385 and H19489.) Interestingly, the EEN-B2-L2 transcript

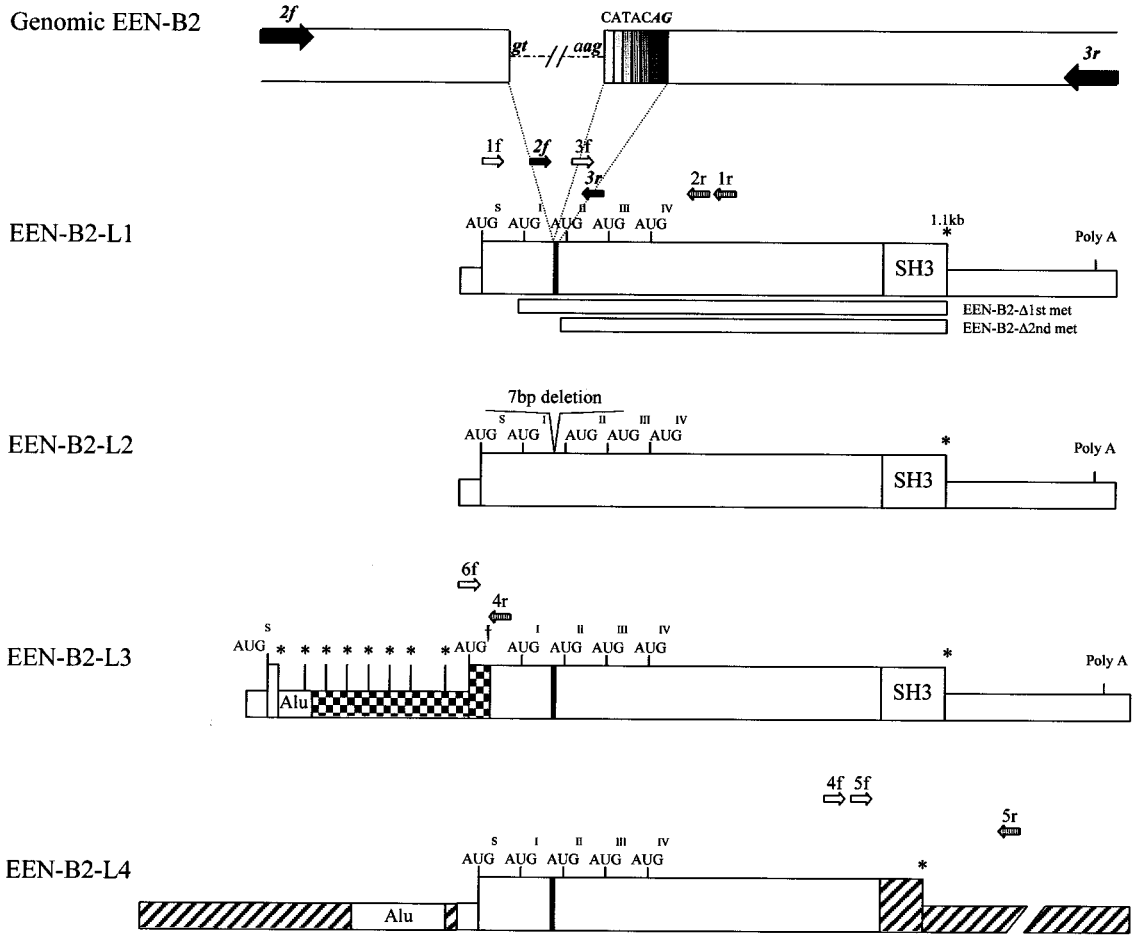

Figure 1 Schematic representation of partial genomic structure and alternatively spliced forms of *EEN-B2* identified in cDNA library screening

The putative start codon and the first four internal methionine codons identified in EEN-B2-L1 are indicated as AUG^{S}, AUG^{I}, AUG^{II}, AUG^{III} and AUG^{IV} respectively. The in-frame-inserted methionine in EEN-B2-L3 is indicated as $AUG^{\dagger}$. Large and small rectangular blocks represent predicted coding sequences and untranslated regions respectively. The thick vertical black line and asterisks indicate the 7-bp mini-exon sequence and stop codons respectively. The chequered- and hatched-shaded boxes represent sequence specific to EEN-B2-L3 and EEN-B2-L4 respectively. The 3.2-kb genomic fragment amplified by *EEN-B2*(2f) and *EEN-B2*(3r) primers is shown on the top. The consensus 3′-splice site, including the 7-bp alternative splice acceptor, is written in block lettering at the top of the diagram. The location of SH3 domains, *Alu* homologous sequences (Alu), polyadenylation signal sites (poly A) and the primers used for PCR analysis [arrows labelled with 1f (forward)–6f and 1r (reverse)–5r] are also shown in the diagram.

could encode an N-terminal-truncated protein retaining the functional SH3 domain if internal methionines (AUG^{II}–AUG^{IV}) downstream of the deletion were utilized as initiation codons. The EEN-B2-L3 transcript differs from EEN-B2-L1 in having a 513-bp fragment with multiple stop codons between the putative starting methionine (AUG^{S}) and the first internal methionine (AUG^{I}) of EEN-B2-L1 (Figure 1). However, the 513-bp insertion would introduce a new in-frame methionine (AUG†), which could be used to make a protein product with a new 22-amino-acid sequence which might replace the first 15 amino acids encoded in EEN-B2-L1. The EEN-B2-L4 transcript was the longest, with additional non-coding sequence at the 5′-end and an alternative 3′-sequence, which would lead to the replacement of the SH3 domain (Figure 1).

Alternative translation initiations for EEN-B2 transcripts

In order to test whether any of the internal methionine codons in EEN-B2 transcripts could be used for translation initiation, *in vitro* transcription and translation assays were performed. The EEN-B2-L1 cDNA clone yielded three protein bands (Figure 2): a faint 40 kDa band that is likely to be initiated from the putative start codon, AUG^{S} (Figure 1), and two strong but smaller protein bands, most likely resulting from initiation from the first and second internal methionine codons (AUG^{I} and AUG^{II} respectively). The use of these two internal methionines was confirmed by testing two types of EEN-B2-L1 cDNA deletion constructs in the assay. With EEN-B2-Δ1st Met (in Figure 1, the EEN-B2-L1 cDNA clone with deletion of 5′ sequence, including the AUG^{S} codon), the two smaller protein bands were produced, whereas only the smallest band was present when EEN-B2-Δ2nd Met (in Figure 1, the EEN-B2-L1 cDNA clone with both AUG^{S} and AUG^{I} deleted) was used (Figure 2). From the intensities of the bands observed, we conclude that AUG^{I} and AUG^{II} function more efficiently than the AUG^{S} codon *in vitro*. When the EEN-B2-L3 cDNA clone was tested, three protein bands of similar intensities were produced; two smaller proteins were initiated from AUG^{I} and AUG^{II}, and the third of approx. 41 kDa was possibly from the new methionine codon AUG† (Figure 1) within the unique 513-bp sequence. When the EEN-B2-L2 cDNA

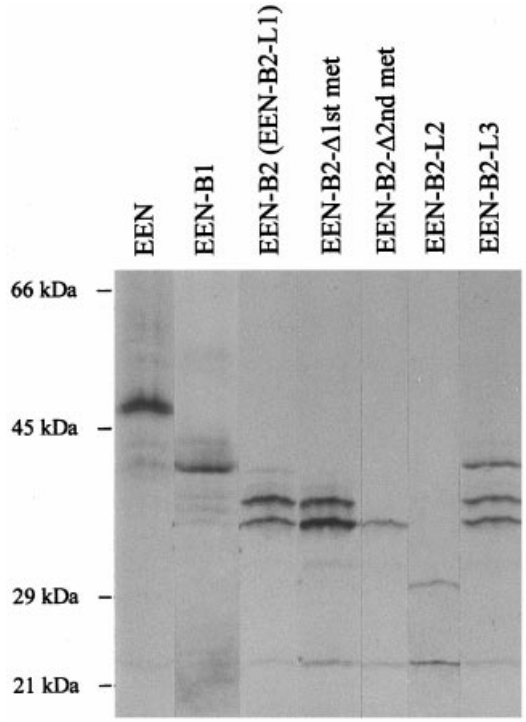

Figure 2 Analysis of protein encoded by different clones of the EEN family

Major protein products with sizes corresponding to those encoded by the longest open reading frame were generated for EEN and EEN-B1 clones. Multiple protein products were produced for EEN-B2 clones. Molecular sizes of the proteins are given in kDa to the left of the gel. The structures of EEN-B2 clones used are shown in Figure 1. EEN-B2-Δ1st met and EEN-B2-Δ2nd met, EEN-B2 with the first or first and second methionines deleted, respectively.

clone was used, a polypeptide of approx. 31 kDa was observed. On the basis of the size of the predicted protein product, this could result from the use of the fourth internal methionine, AUG^{IV}, as an initiation codon. We believe that the preferential use of the fourth internal methionine as the initiation codon is the result of a better match to the ACCATGG Kozak consensus sequence [34]. There is also a weak 23-kDa band from EEN-B2-derived transcripts that could be an N-terminal-truncated product upon utilization of an internal initiation codon. Together with the alternative splicing patterns of the *EEN-B2* gene, our data indicate the presence of complex regulation of the *EEN-B2* gene at the levels of both transcription and translation. In contrast, EEN and EEN-B1 cDNAs generate only a single major protein product corresponding to the longest open reading frame (Figure 2), although these four internal in-frame methionines of EEN-B2 are conserved in EEN and EEN-B1 sequences.

Amplification of EEN-B2 transcripts (-L1 to -L4) from human brain tissues

To study the expression of EEN-B2 variants in human brain, PCR amplification was performed with specific primers for each transcript in normal adult and fetal brain, and medulloblastoma (Figure 3A). Transcript-specific primer pairs for *EEN-B2*-L3 and *EEN-B1* resulted in the amplification of RNA transcripts from all three samples, but not in the control genomic DNA. The *EEN-B2*(1f) and *EEN-B2*(2r) primer pair, which flanked the 7-bp deletion identified in EEN-B2-L2, resulted in the amplification of doublets from the brain samples. Sequence analysis showed that the lower band of 372 bp was derived from the EEN-B2-L2 transcript, which had a 7-bp deletion, whereas the upper band of 379 bp was amplified from EEN-B2-L1 (Figure 3A), confirming the presence of these two transcripts. However, EEN-B2-L4-specific primers did not generate a PCR product, indicating that the cDNA clone might represent an incompletely processed form of EEN-B2.

EEN-B2-L2 is generated using an alternative 3′-splice acceptor site

In order to distinguish whether EEN-B2-L2 was derived from alternative splicing of EEN-B2-L1 or from a separate *EEN-B2*-like gene, PCR analysis was performed on human genomic DNA using another pair of transcript-specific primers, *EEN-B2*(2f) and *EEN-B2*(3r), flanking the 7-bp deletion of EEN-B2-L2 (Figure 1). A DNA fragment of 3.2 kb was amplified and sequenced. Comparison of the DNA sequences of this fragment with the EEN-B2-L1 cDNA indicated the presence of a 3.1-kb intron with perfect 5′- and 3′-splice sites at the junctions (GT-AG consensus) (Figure 1). At the 3′-splice site, the sequence was a*ag*/CATAC*AG*/ (potential 3′-cryptic splice sites are shown underlined and in italics), suggesting that there are two potential alternative splice junctions (Figure 1), of which the second with a 5′ cytosine (C) could be preferred to the first one with adenosine (A) in front of the consensus AG splice sequence. This is also consistent with the scanning model of RNA splicing [35], and suggests that differential splicing at these two sites would produce two transcripts differing by 7 bp. Thus the EEN-B2-L2 transcript is likely to be an alternatively spliced form that is 7 bp shorter than EEN-B2-L1.

Expression of EEN-B1 and EEN-B2 transcripts is spatially and temporally specific

The expression of EEN, EEN-B1 and EEN-B2 was examined in Northern blots of poly(A)$^+$ RNA from different human and mouse tissues (Figure 3B), as well as by reverse transcriptase (RT)-PCR analysis on human multiple tissue cDNA panels (Figure 3C). In contrast with EEN mRNA, which was expressed ubiquitously in all adult tissues tested, EEN-B1 and -B2 mRNAs were preferentially expressed in brain and testis of adult mice, with higher levels of EEN-B1 mRNA expression in the brain and higher levels of EEN-B2 mRNA signal in the testis. Within the central nervous system (CNS), EEN-B2 and EEN mRNA were both expressed at a high level in most parts of the brain and spinal cord, whereas EEN-B1 mRNA is preferentially expressed in regions enriched in neurons, including cerebral and cerebellar cortex, occipital lobe, frontal lobe and temporal lobe, but only at a very low level in the spinal cord, corpus callosum and subthalamic nucleus. Using RT-PCR analysis, EEN-B1 was found to be expressed weakly in most non-neuronal tissues, but not in adult colon or leucocytes (Figure 3C).

EEN-B2 variant transcripts were differentially expressed in various tissues

To investigate whether the various EEN-B2 transcripts were differentially expressed, PCR analysis was performed using primers specific for individual EEN-B2 transcripts. When *EEN-B2*(1f) and *EEN-B2*(2r) primers were used, doublets were amplified from all the tissues in which these transcripts were expressed, including adult brain, testis and thymus. In each doublet, the intensity of the smaller band, corresponding to EEN-B2-L2, was much weaker (Figure 3C). Using EEN-B2-L3 transcript-specific primers, the tissue distribution of the EEN-B2-L3 transcript was

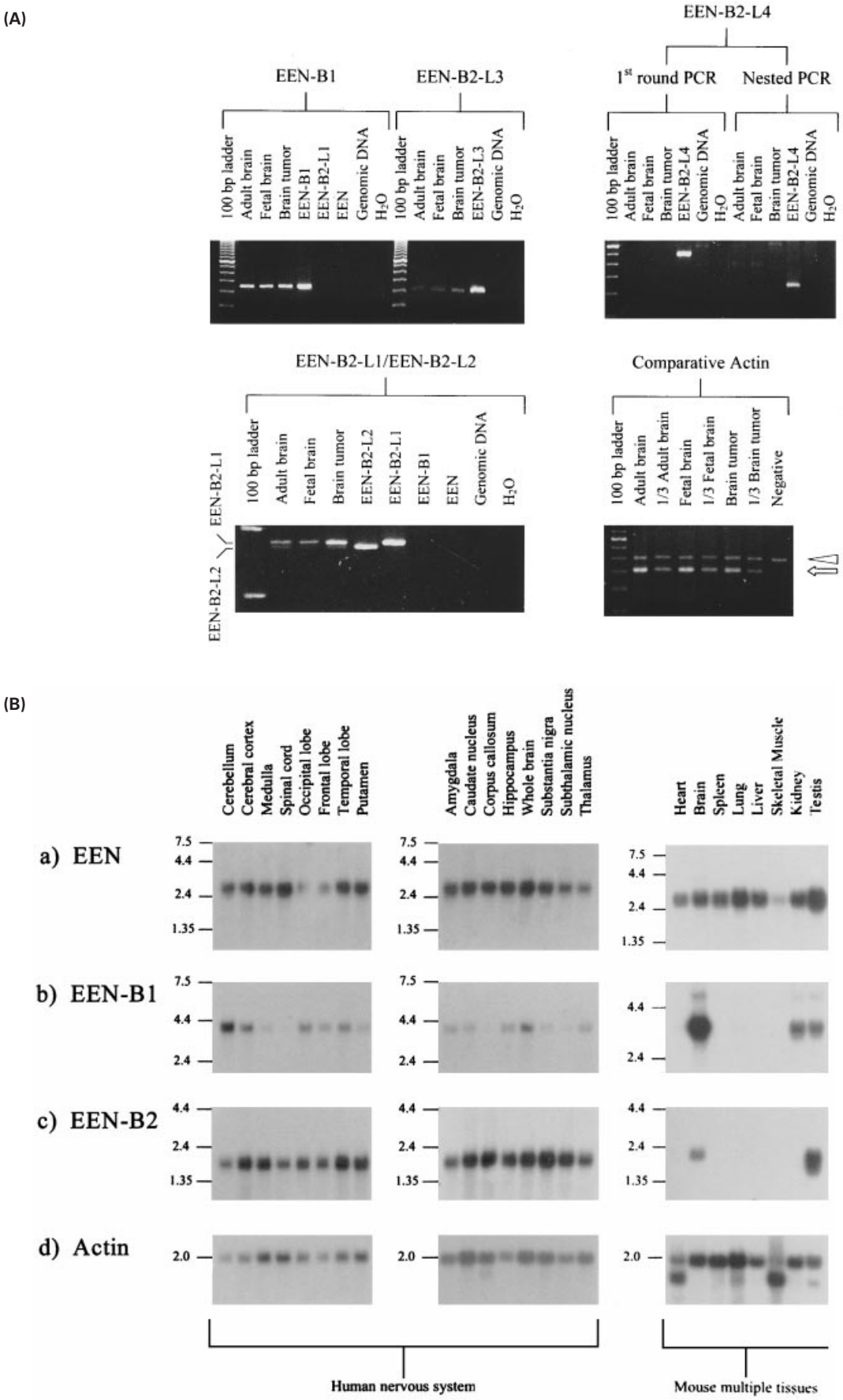

Figure 3 For legend see facing page.

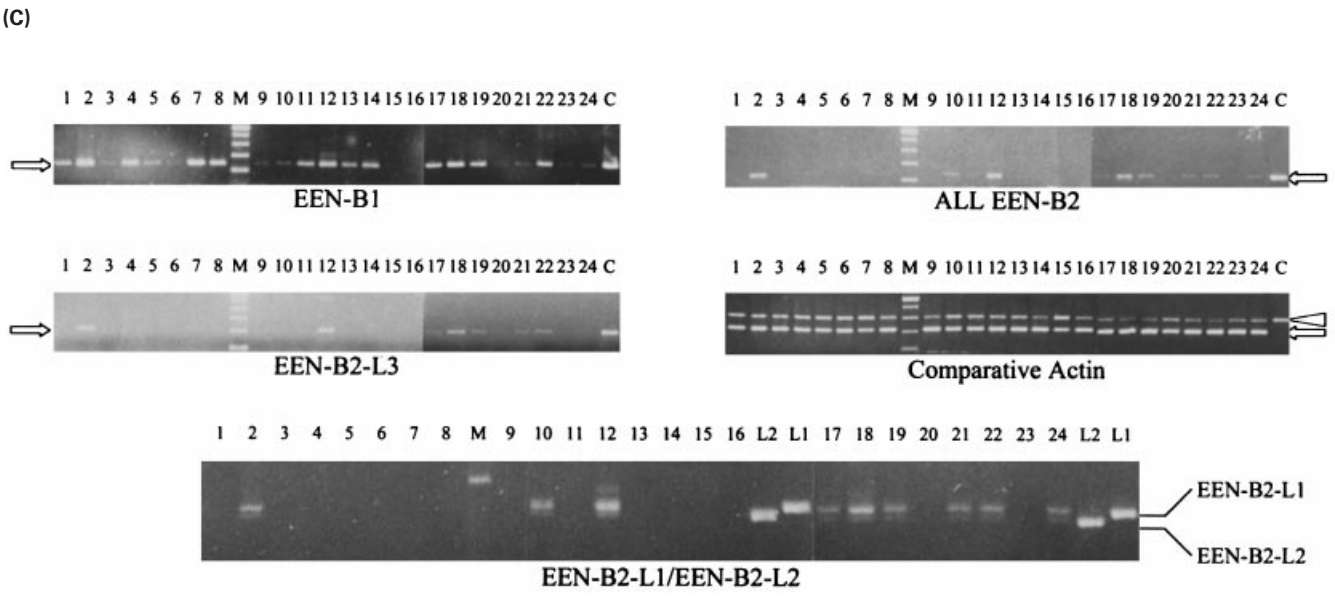

Figure 3 Expression analysis of *EEN* family in human and mouse tissues

(**A**) PCR amplification of EEN-B1 and -B2 variant transcripts from various human brain tissues. Transcripts that were amplified are indicated above the brackets. cDNA templates (i.e. EEN, EEN-B1 and EEN-B2-L1–L4) and genomic DNA were used as positive and negative controls respectively for each amplification. The relative positions of EEN-B2-L1 and EEN-B2-L2 transcripts are indicated to the left of the bottom left gel in (**A**). In the comparative actin PCR, the arrowhead indicates the control actin band amplified from internal control plasmid DNA, whereas the arrow indicates the actin amplified from the cDNA samples. Actin PCR was also performed using a 3-fold dilution of the cDNA templates. (**B**) Northern blot analysis of the EEN family in the human nervous system (left and centre panels of gels) and mouse multiple tissues (right panel of gels). These blots were hybridized with human and mouse probe (see the Experimental section). Each blot was normalized with actin hybridization. Molecular sizes of RNA fragments are given in kb. (**C**) Differential expression of EEN-B1 and -B2 splice variants assessed by PCR analysis on multiple tissue cDNA panels. The transcripts that were amplified are indicated at the bottom of each panel. 'ALL EEN-B2' represents the amplification of EEN-B2-L1–L3 transcripts. Arrows indicate specific products amplified from the samples; the arrowhead to the right of the ALL EEN-B panel indicates the control actin band amplified from the internal control plasmid DNA, as shown in (**A**). 1, adult heart; 2, adult brain; 3, placenta; 4, adult lung; 5, adult liver; 6, adult skeletal muscle; 7, adult kidney; 8, adult pancreas; 9, adult spleen; 10, adult thymus; 11, adult prostate; 12, adult testis; 13, adult ovary; 14, adult small intestine; 15, adult colon; 16, adult peripheral blood leucocyte; 17, fetal heart; 18, fetal brain; 19, fetal lung; 20, fetal liver; 21, fetal skeletal muscle; 22, fetal kidney; 23, fetal spleen; 24, fetal thymus; c, control plasmid DNA; M, 100-bp ladder marker.

similar to the overall EEN-B2 expression pattern (Figure 3C, ALL EEN-B2), except that EEN-B2-L3 transcripts were present in neither adult nor fetal thymus. No signal could be amplified from any of the tissues using EEN-B2-L4-specific primers (results not shown), suggesting that this transcript is not normally expressed in those tissues that were tested.

Expression of the *EEN* family in mouse embryos

To examine the expression patterns of *EEN* family members during embryonic development, whole-mount and section ISHs of mouse embryos were performed using riboprobes transcribed from the murine homologues of the *EEN* family [4]. The murine *EEN* was widely distributed in 8.5 dpc mouse embryos and by 9.5 dpc, high levels of expression were detected throughout the entire embryo (Figures 4A and 4B). This expression pattern persisted in later-stage embryos (10.5, 12.5 and 14.5 dpc), as shown in Figures 4(G), 4(L) and 4(Q). Therefore the murine EEN mRNA appears to be expressed ubiquitously during embryonic development.

The expression patterns of murine EEN-B1 and EEN-B2 mRNA were very similar, and their onset of expression was much later than that of murine EEN. No expression could be detected in 8.5 or 9.5 dpc embryos by whole-mount ISH (Figures 4D and 4E). However, by 10.5 dpc, both murine EEN-B1 and EEN-B2 messages were observed, and their expression appeared to be confined to the developing CNS, including various parts of brain (throughout the telencephalon, mesencephalon, metencephalon and myelencephalon) and spinal cord (Figures 4H and 4I). The expression for these two genes at this stage appeared to be stronger in the ventral region of the CNS. In addition, vascular structures, such as dorsal aorta and the epithelial surface of the branchial arches, also expressed the EEN-B1 and -B2 mRNA. At 12.5 dpc, the signals detected in the developing CNS were uniform and stronger: almost all neurons in the spinal cord and brain expressed EEN-B1 and EEN-B2. Hybridization signals could also be found in tissues of the peripheral nervous system. High levels of EEN-B1 and EEN-B2 mRNA expression were seen in the outermost layer of the cortical plate in the telencephalon (cortical neuroepithelium), as well as spinal ganglia. At the same time, weak signals were also detected in some non-neuronal tissues, including kidney, intestine and lung (Figures 4M and 4N). At 14.5 dpc, EEN-B1 and EEN-B2 mRNAs were strongly expressed in all neurons of the CNS, including the olfactory bulb. Signals can also be seen in the cranial ganglia of the developing nervous system, and in the developing cochlea (Figures 4R and 4S). At this stage, the expression levels of EEN-B1 and EEN-B2 in non-neuronal tissues, including kidney, adrenal medulla, intestine and lung, were remarkably higher than that at 12.5 dpc.

Expression of EEN family members in mouse adult brain and testis

To examine in more detail the expression of *EEN* family members in adult tissues, ISH on mouse tissue sections revealed that EEN-B1 and EEN-B2 mRNAs were widely expressed throughout the adult brain, including the cerebral cortex, hippocampus, cer-

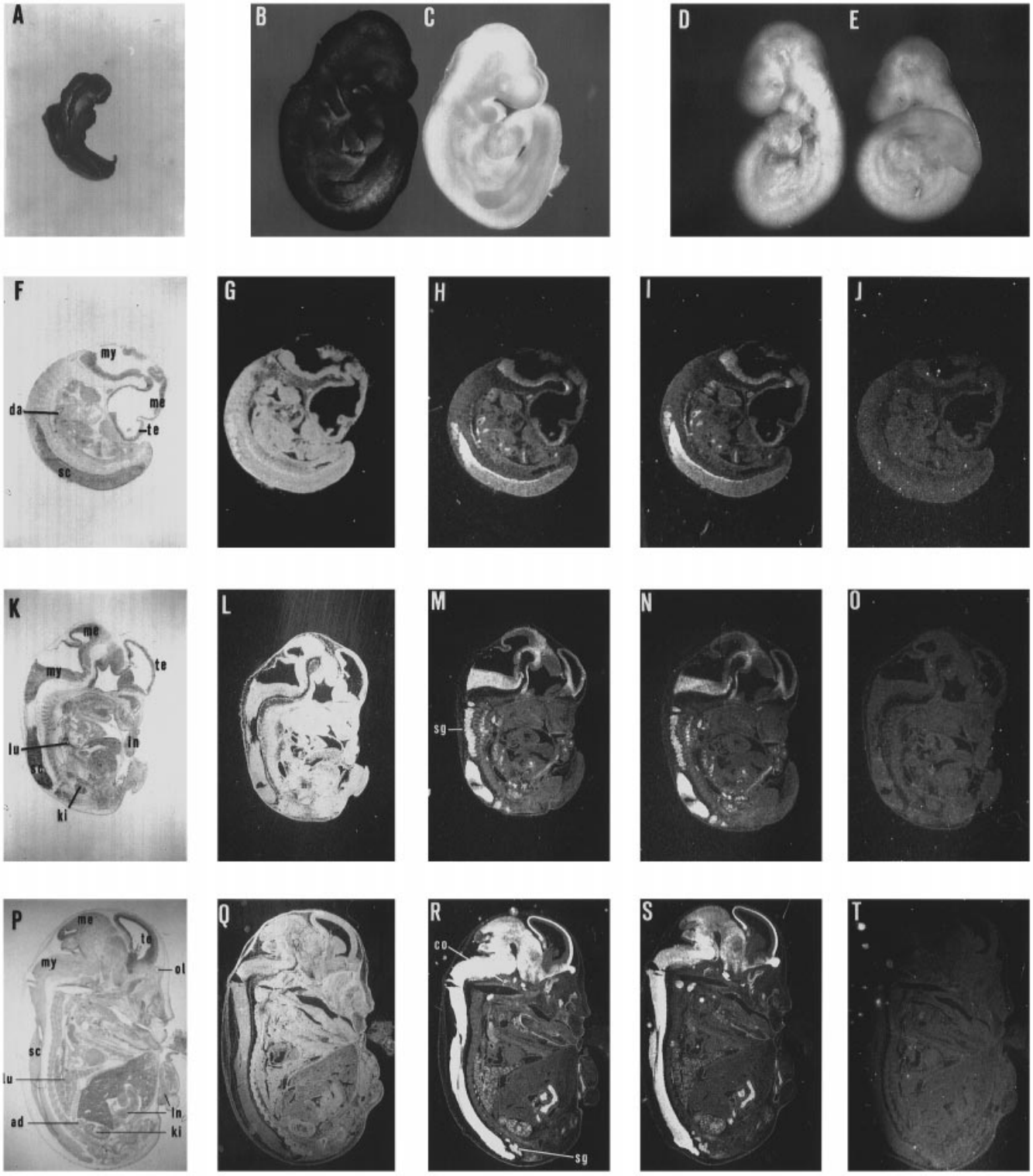

Figure 4 Temporal and spatial patterns of EEN family expression during mouse embryonic development by ISH

Whole-mount mouse embryos of 8.5 (**A**) and 9.5dpc (**B**–**E**) were hybridized with digoxigenin-labelled mouse EEN antisense probe (**A**, **B**), EEN sense probe (**C**), EEN-B1 antisense probe (**D**) and EEN-B2 antisense probe (**E**) respectively. Mouse embryos of 10.5 (**F**–**J**), 12.5 (**K**–**O**) and 14.5 dpc (**P**–**T**) were sectioned and hybridized with ^{35}S-radiolabelled mouse EEN antisense probe (**G**, **L** and **Q**), EEN-B1 antisense probe (**H**, **M** and **R**) or EEN-B2 antisense probe (**I**, **N** and **S**) respectively. All EEN, EEN-B1 and EEN-B2 probes exhibited similar results on sense probe hybridization; only the EEN sense probe (**J**, **O** and **T**) was shown. Bright fields of 10.5, 12.5 and 14.5 dpc embryos were shown as (**F**), (**K**) and (**P**) respectively. ad, adrenal medulla; co, cochlea; da, dorsal aorta; in, intestine; ki, kidney; lu, lung; me, mesencephalon; mt, metencephalon; my, myelencephalon; ol, olfactory bulb; sc, spinal cord; sg, spinal ganglia; te, telencephalon.

ebellum, brain stem, thalamus and striatum (Figures 5C and 5D). Highest levels of expression were detected in regions with high neuronal density, such as the cerebral cortex, cerebellum, the dentate gyrus and pyramidal cell layer of the hippocampal formation. Morphological appearance of cells showing hybridization signals suggested that both EEN-B1 and EEN-B2 are expressed in neurons; the expression pattern of EEN in adult brain was similar to that of EEN-B1 and EEN-B2, with expression predominantly occurring in the grey matter, except for a low level of EEN expression that was detected in the white matter and the epithelium of the choroid plexus (Figure 5B).

In the hippocampus, the expression of EEN-B1 and EEN-B2 in pyramidal cells CA3 was much stronger that in CA1, CA2, CA4 and dentate gyrus (Figures 5G and 5H); whereas EEN mRNA showed a similar level of expression in pyramidal cells of CA1 to CA4, and the dentate gyrus (Figure 5F). In the cerebral cortex, the expression of EEN family members were restricted to the neuronal cells of the granular layer, and were not found in the molecular layer (Figures 5J–5L). Similar expression patterns were also found in cerebellar cortex, with predominant expression in cerebellar granular layer and Purkinje cells and weak signals in the molecular layer (Figures 5N–5P). Although the striatum has a low neuronal density, cells in striatum with morphological characteristics consistent with neurons expressed high levels of EEN-family-member mRNAs, whereas glial cells did not (Figures 5R–5U).

Besides the adult brain, testis is the only mouse tissue where the three EEN family members are co-expressed (Figure 3B). ISH revealed that all EEN family members were highly expressed in seminiferous tubules in the testis (Figures 5V–5X). High magnification revealed that EEN-B1 and EEN-B2 were expressed in the basal lamina of the seminiferous epithelium, containing Sertoli cells and immature spermatogonia, whereas EEN was predominantly expressed in the primary and secondary spermatocytes, although weak EEN expression could also be seen in Sertoli cells and Leydig cells (Figures 5AA–5CC). The expression of EEN family members in Sertoli cells has been confirmed further by RT-PCR analysis using RNA extracted from primary Sertoli cell culture of purity $> 98\%$, prepared as described previously ([36], and results not shown).

EEN family members and amphiphysin compete for synaptojanin and dynamin

To assess the relative binding affinity of individual members of the EEN family to their potential interacting partners, synaptojanin and dynamin, various amounts (1–50 μg) of SH3-domain proteins derived from EEN family members (EEN and EEN-B1) were used as competitors to compete with different GST fusion proteins containing the SH3 domains of EEN family members for binding with ^{35}S-labelled synaptojanin and dynamin. Since similar results were obtained using synaptojanin or dynamin as input; we only show here the result with synaptojanin. As shown in Figure 6(a), B1-SH3 protein could readily compete with both GST–EEN-SH3 and GST–B2-SH3 fusion proteins for binding with synaptojanin, indicating that B1-SH3 protein has a higher affinity for synaptojanin and dynamin compared with EEN and EEN-B2. On the other hand, EEN-SH3 protein could compete only with GST–B2-SH3, and not with GST–B1-SH3, for binding with synaptojanin and dynamin, whereas B2-SH3 could not inhibit any binding of GST-EEN-SH3 or GST-B1-SH3 (results not shown). These inhibitions were unlikely to be due to non-specific binding, since no inhibition was found using 50 μg of RasGAP-SH3 protein, which exhibits a different binding specificity. The competition results suggested that the binding affinity of EEN family members to synaptojanin and dynamin, in order of decreasing affinity, was EEN-B1 $>$ EEN $>$ EEN-B2.

Since members of the EEN family, amphiphysin, synaptojanin and dynamin have overlapping domains of expression in the neural tissues, we wanted to identify whether EEN family members and amphiphysin could compete under normal circumstances for binding with synaptojanin and dynamin. Since the SH3 domains of amphiphysin I and II are known to bind to the same PRD on dynamin [37], they were used as a positive control in the protein competitive-binding assay. We showed that amphiphysin I-SH3 protein could efficiently compete with GST–amphiphysin-II-SH3 fusion protein for synaptojanin when 25 μg of competitor protein was used (Figure 6b). When amphiphysin-I-SH3 protein competed with GST–EEN family proteins, inhibition could be seen using $< 50\ \mu$g of competitor protein (Figure 6b). Similar results were obtained using dynamin as the input (results not shown). Inhibition was not found using 50 μg of RasGAP-SH3 protein. Our results suggested that, in terms of binding affinity, amphiphysin could compete with EEN family members for binding with synaptojanin and dynamin.

DISCUSSION

The EEN family belongs to the group of SH3-domain-containing proteins, which have been implicated in many biochemical processes, including cell proliferation and differentiation, cell architecture, protein trafficking and subcellular localization, as well as the immune response to infection (for a review, see [38]). Studies *in vitro* and *in vivo* have shown that the EEN family is now known to interact with dynamin, synaptojanin, endocytic proteins involved in endocytosis [1,2] and leukaemia [3], as well as with HD, which is implicated in Huntington's disease [25]. There are few data, however, in existence comparing the expression of the EEN family in various mouse and human tissues with that reported for dynamin, synaptojanin and HD, or from binding studies, which may reveal further insights into how the EEN family mediates various cellular functions.

Using the combination of Northern blot analysis, RT-PCR and ISH, we have shown that the EEN family members, despite high sequence and structural similarities, have distinctive but overlapping expression domains. Our data show that EEN is ubiquitously expressed in most tissues, whereas EEN-B1 is expressed mainly in adult brain and EEN-B2 is expressed in both the brain and the testis. Within the brain, the expression of EEN-B1 and EEN-B2 in the brain is highest in the neurons of the granular layer of the cerebral cortex, the internal granules and Purkinje cells of cerebellar cortex and hippocampus; these expression patterns are parallel with those reported for dynamin-I/III [28,39] and synaptojanin-I [40]. In the testis, EEN-B1 and EEN-B2, like testis-type dynamin, i.e. dynamin-III [29,41], are preferentially expressed in the Sertoli cells, which are known to elaborate endocytic processes and nurse developing germ cells. Taken together, our results support a role for the EEN family members in endocytosis in both the brain and the testis. We also show that EEN family members are not functionally redundant, and might act in different tissues at different developmental stages. This is apparent from the expression patterns of EEN-B1 and EEN-B2; both are expressed similarly in mouse embryos, whereas in the adult stage only EEN-B1 is expressed in the mouse adult kidney.

Our detailed studies in the brain have revealed two unexpected findings. First, there is intense expression of EEN-B1 and -B2 in the CA3 area of the hippocampus; this is the same region where dynamin and synaptojanin are highly expressed. To date, very

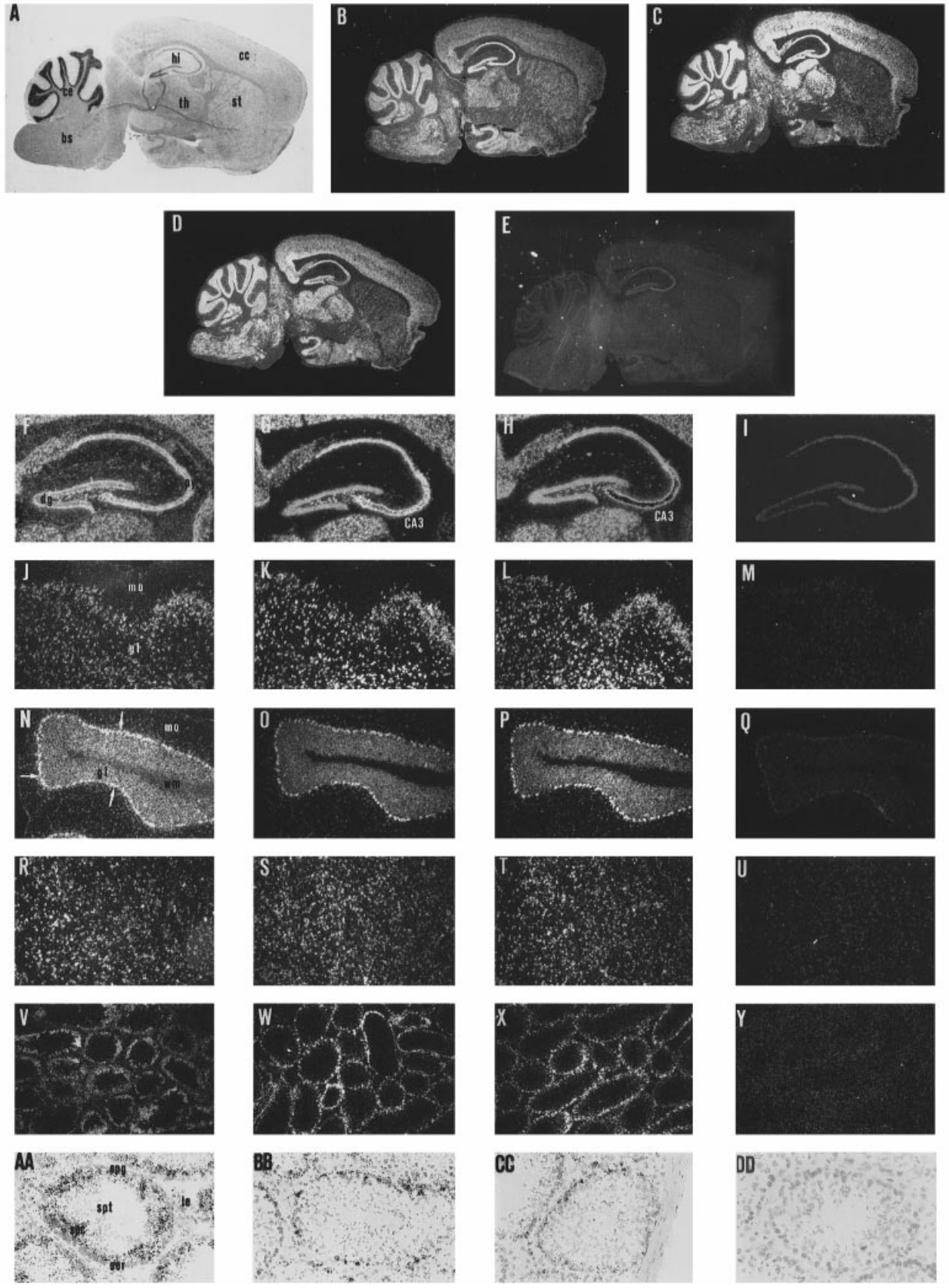

Figure 5 Expression of EEN family members in adult brain (A–U) and testis (V–Y, and AA–DD)

Sagittal sections of mouse brain (**A**–**E**) were hybridized with ^{35}S-radiolabelled mouse antisense probe of EEN (**B**), EEN-B1 (**C**), EEN-B2 (**D**) and sense probe of EEN (**E**). Photomicrographs of emulsion-dipped sections of hippocampal formation (**F**–**I**), cerebral cortex (**J**–**M**), cerebellar cortex (**N**–**Q**), striatum (**R**–**U**) and testis (**V**–**Y** and **AA**–**DD**) that were hybridized with antisense probes

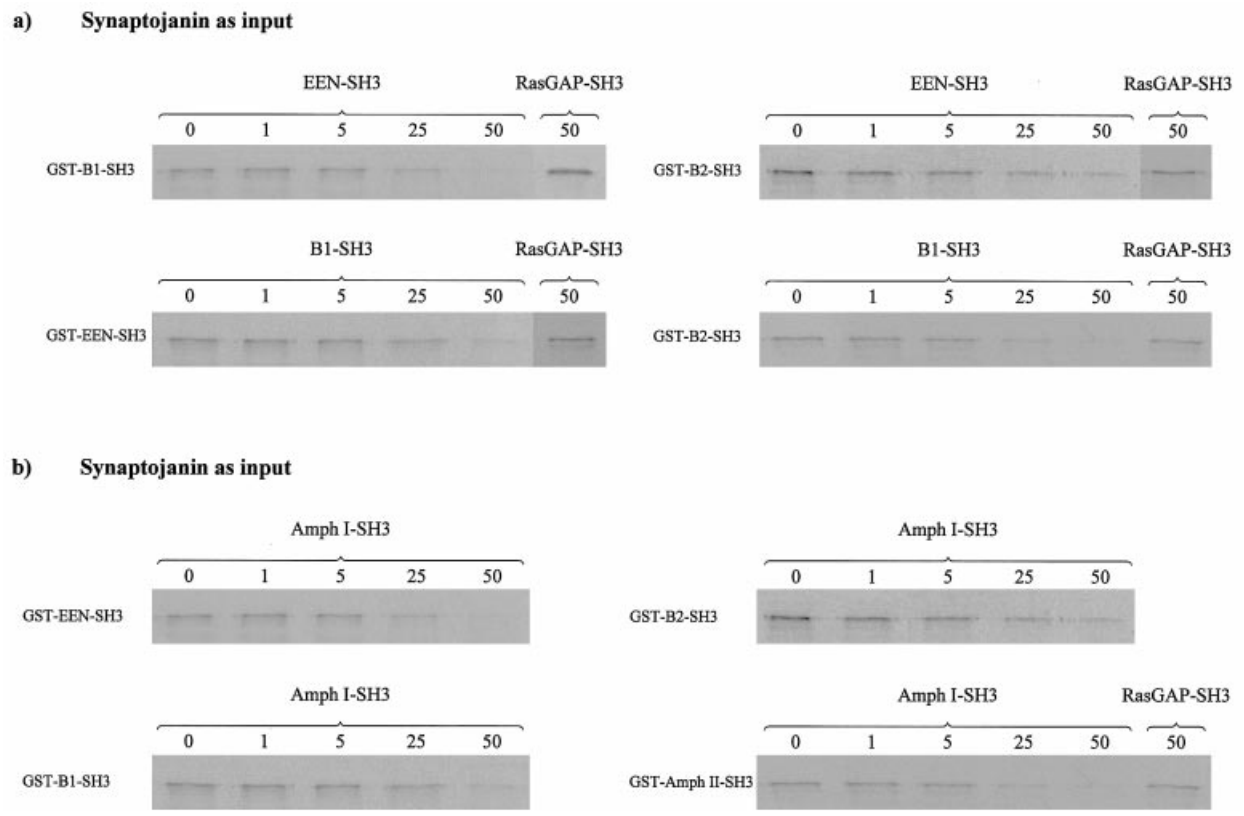

Figure 6 Competitive binding assay of synaptojanin among members of the EEN family and amphiphysin

(**a**) Top panels: immobilized GST fusion proteins of B1-SH3 (left) and B2-SH3 (right) were incubated with ^{35}S-labelled synaptojanin-145 in the presence of 0, 1, 5, 25 or 50 μg of EEN-SH3 protein respectively. Bottom panels: immobilized GST fusion proteins of EEN-SH3 (left) and B2-SH3 (right) were incubated with ^{35}S-labelled synaptojanin-145 in the presence of 0, 1, 5, 25 or 50 μg of B1-SH3 protein respectively. (**b**) Immobilized GST fusion proteins of EEN-SH3 (top left), B1-SH3 (bottom left), B2-SH3 (top right), and amphiphysin II (Amph II)-SH3 domains (bottom right) were incubated with ^{35}S-labelled synaptojanin-145 in the presence of 0, 1, 5, 25 or 50 μg of amphiphysin I (Amph I)-SH3 protein respectively. The negative controls using 50 μg RasGAP-SH3 protein are also indicated for (**a**) and (**b**). Similar results were obtained using dynamin as the input (results not shown).

few numbers of molecules that discriminate between sub-populations of hippocampal cells have been identified [42]. The significance of the finding that these four different molecules are predominantly co-expressed in the CA3 area of the hippocampus is unclear; one possibility is that they might play a role in mediating the specific synaptic functions of this discrete area in the hippocampus. Secondly, we have found that EEN-B1/-B2 and HD share similar expression patterns in both adult and fetal tissues [43–47]. Taken together with the observation that EEN-B2 has been found to interact with the glutamine expansion region of the HD protein and promotes the formation of insoluble polyglutamine-containing aggregates [25], our findings suggest a link between the pathogenesis of Huntington's disease and the association of HD with EEN family members.

In our study, we have also identified three different spliced variants of EEN-B2 (L1 to L3), which all contain a C-terminal SH3 domain. EEN-B2-L1 and EEN-B2-L2 possess identical expression patterns, whereas EEN-B2-L3 is expressed only in adult brain and testis, and not in the thymus, where L1 and L2 can be detected. Interestingly, the recent study on dynamin in rat tissues using RT-PCR has also identified multiple-spliced variants with different tissue specificity [31]. Most of these dynamin variants can be found in adult brain, but not in epithelial-based tissues, except in the testis, where over half of the splice variants of dynamin II and III can be detected. One could speculate that splice variants of the EEN family and dynamin may be targeted to different cellular compartments in order to carry out their functions. This speculation is consistent with a recent study on Intersectin, a newly identified SH3-domain-containing protein with an affinity for dynamin, in which different splice variants of Intersectin with specific tissue distribution were shown to be components of the endocytic machinery in neurons and non-neuronal cells respectively [48].

We have shown that, within the EEN family, the binding affinity of EEN-B1 to synaptojanin and dynamin is higher than that of EEN and EEN-B2. Accordingly, EEN-B1 will preferentially interact with synaptojanin in the cells (e.g. in neurons) co-expressing other EEN family members. This result is consistent with the finding of EEN-B1/endophilin I as being the major synaptojanin-binding protein in rat brain [1]. However, competition *in vitro* can only be seen with large amounts of competitor proteins (e.g. 50 μg).

of EEN (**F**, **J**, **N**, **R**, **V**, **AA**), EEN-B1 (**G**, **K**, **O**, **S**, **W**, **BB**) and EEN-B2 (**H**, **L**, **P**, **T**, **X**, **CC**) and EEN sense probes (**I**, **M**, **Q**, **U**, **Y**, **DD**) respectively. bs, brain stem; cc, cerebral cortex; ce, cerebellum; dg, dentate gyrus; gl, granular layer; hi, hippocampus; le, Leydig cells; mo, molecular layer; py, pyramidal cell layer of the hippocampal formation; ser, Sertoli cells; spc, spermatocytes; spg, spermatogonia; spt, spermatids; st, striatum; th, thalamus; wm, white matter. Arrows (white) indicate the Purkinje cells in (**J**). CA3, a type of pyramidal cell of the hippocampus.

The possible role of the EEN family in clathrin-mediated endocytosis has been demonstrated by the recent finding of lysophosphatidic acid acyltransferase (LPAAT) activity of EEN-B1/endophilin I [49]. The LPAAT activity of EEN-B1 converts an 'inverted-cone-shaped' lipid into a cone-shaped lipid, and induces membrane curvature, which leads to the formation of synaptic-like microvesicles (SLMVs). A C-terminal EEN-B1 mutant lacking the dynamin/synaptojanin-binding SH3 domain, but still retaining LPAAT activity, was defective in the formation of SLMVs [49,50]. These findings demonstrated that protein–protein interaction of EEN-B1 via its SH3 domain is essential for mediating the formation of SLMVs. In addition to the EEN family, the SH3 domain of amphiphysin also binds specifically to dynamin and synaptojanin in the presynaptic termini. Using peptide-competition assays, we demonstrate that amphiphysin I will prevent EEN family members from binding to synaptojanin and dynamin. This inhibition possibly resulted from the steric effect of these two proteins binding, since EEN family proteins and amphiphysin bind to two adjacent PRDs on synaptojanin ([51,52]; C. W. So and L. C. Chan, unpublished work). Previous studies *in vivo* [53] have shown that synaptojanin can form two separate and stable complexes in the nerve terminal, i.e. (i) synaptojanin with EEN-B1, and (ii) synaptojanin with amphiphysin and dynamin. Our finding of competitive binding between the EEN family members and amphiphysin suggest that amphiphysin may regulate the amount of synaptojanin and/or dynamin at the sites of endocytosis by controlling the availability of these proteins for the EEN family. Further studies *in vivo* involving the overexpression of wild-type and mutant proteins of amphiphysin and EEN family members may help to address this possibility.

We thank Brian Kay for providing murine cDNA of the EEN family, P. De Camilli for providing cDNA of dynamin and synaptojanin, H. T. McMahon for GST–Grb2 fusion cDNA and constructive advice, W. M. Lee for provision of cDNA from purified Sertoli cells, and Stanley Ko for technical support. This work was funded by RGC grant 338-046-0009.

REFERENCES

1 De Heuvel, E., Bell, A. W., Ramjaun, A. R., Wong, K., Sossin, W. S. and McPherson, P. S. (1997) J. Biol. Chem. **272**, 8710–8716
2 Ringstad, N., Nemoto, Y. and De Camilli, P. (1997) Proc. Natl. Acad. Sci. U.S.A. **94**, 8569–8574
3 So, C. W., Caldas, C., Liu, M.-M., Chen, S.-J., Huang, Q.-H., Gu, L.-J., Sham, M. H., Wiedemann, L. M. and Chan, L. C. (1997) Proc. Natl. Acad. Sci. U.S.A. **94**, 2563–2568
4 Sparks, A. B., Hoffman, N. G., McConnell, S. J., Fowlkes, D. M. and Kay, B. K. (1996) Nat. Biotechnol. **14**, 741–744
5 Giachino, C., Lantelme, E., Lanzetti, L., Saccone, S., Della Valle, G. and Migone, N. (1997) Genomics **41**, 427–434
6 Chen, M. S., Obar, R. A., Schroeder, C. C., Austin, T. W., Poodry, C. A., Wadsworth, S. C. and Vallee, R. B. (1991) Nature (London) **351**, 583–586
7 van der Bliek, A. M. and Meyerowitz, E. M. (1991) Nature (London) **351**, 411–414
8 Kosaka, T. and Ikeda, K. (1983) J. Cell Biol. **97**, 499–507
9 Ramaswami, M., Krishnan, K. S. and Kelly, R. B. (1994) Neuron **13**, 363–375
10 Hinshaw, J. E. and Schmid, S. L. (1995) Nature (London) **374**, 190–192
11 Takei, K., McPherson, P. S., Schmid, S. L. and De Camilli, P. (1995) Nature (London) **374**, 186–190
12 McPherson, P. S., Garcia, E. P., Slepnev, V. I., David, C., Zhang, X., Grabs, D., Sossin, W. S., Bauerfeind, R., Nemoto, Y. and De Camilli, P. (1996) Nature (London) **379**, 353–357
13 De Camilli, P., Emr, S. D., McPherson, P. S. and Novick, P. (1996) Science **271**, 1533–1539
14 Mayinger, P., Bankaitis, V. A. and Meyer, D. I. (1995) J. Cell Biol. **131**, 1377–1386
15 Singer-Krüger, B., Nemoto, Y., Daniell, L., Ferro-Novick, S. and De Camilli, P. (1998) J. Cell Sci. **111**, 3347–3356
16 Wigge, P. and McMahon, H. T. (1998) Trends Neurosci. **21**, 339–343
17 Lichte, B., Veh, R. W., Meyer, H. E. and Kilimann, M. W. (1992) EMBO **11**, 2521–2530
18 David, C., McPherson, P. S., Mundigl, O. and De Camilli, P. (1996) Proc. Natl. Acad. Sci. U.S.A. **93**, 331–335
19 Robinson, M. S. (1994) Curr. Opin. Cell Biol. **6**, 538–544
20 Munn, A. L., Stevenson, B. J., Geli, M. I. and Riezman, H. (1995) Mol. Biol. Cell **12**, 1721–1742
21 Shupliakov, O., Löw, P., Grabs, D., Gad, H., Chen, H., David, C., Takei, K., De Camilli, P. and Brodin, L. (1997) Science **276**, 259–263
22 Wigge, P., Vallis, Y. and McMahon, H. T. (1997) Curr. Biol. **7**, 554–560
23 Urrutia, R., Henley, J. R., Cook, T. and McNiven, M. A. (1997) Proc. Natl. Acad. Sci. U.S.A. **94**, 377–384
24 Schmid, S. L., McNiven, M. A. and De Camilli, P. (1998) Curr. Opin. Cell Biol. **10**, 504–512
25 Sittler, A., Wälter, S., Wedemeyer, N., Hasenbank, R., Scherzinger, E., Eickhoff, H., Bates, G. P., Lehrach, H. and Wanker, E. E. (1998) Mol. Cell **2**, 427–436
26 Zechner, U., Scheel, S., Hemberger, M., Hopp, M., Haaf, T., Fundele, R., Wanker, E. E., Lehrach, H., Wedemeyer, N. and Himmelbauer, H. (1998) Genomics **54**, 505–510
27 Sharp, A. H., Love, S. J., Schilling, G., Li, S. H., Li, X. J., Bao, J., Wagster, M. V., Kotzuk, J. A., Steiner, J. P., Lo, A. et al. (1995) Neuron **14**, 1065–1074
28 Sontag, J.-M., Fykse, E. M., Ushkaryov, Y., Liu, J.-P., Robinson, P. J. and Südhof, T. C. (1994) J. Biol. Chem. **269**, 4547–4554
29 Cook, T., Mesa, K. and Urrutia, R. (1996) J. Neurochem. **67**, 927–931
30 Nemoto, Y., Arribas, M., Haffner, C. and De Camilli, P. (1997) J. Biol. Chem. **272**, 30817–30821
31 Cao, H., Garcia, F. and McNiven, M. A. (1998) Mol. Biol. Cell **9**, 2595–2609
32 Ausubel, F. M., Brent, R., Kingston, R. E., Moore, D. D., Seidman, J. G., Smith, J. A. and Struhl, K. (1987) Current Protocols in Molecular Biology, pp. 6.0.1–6.12.12 (suppl. 27), John Wiley & Sons, New York
33 Sham, M. H., Vesque, C., Nonchev, S., Marshall, H., Frain, M., Gupta, R. D., Whiting, J., Wilkinson, D., Charnay, P. and Krumlauf, R. (1993) Cell **72**, 183–196
34 Kozak, M. (1996) Cell **44**, 283–292
35 Sharp, P. A. (1981) Cell **23**, 643–646
36 Chung, S. S., Zhu, L. J., Mo, M. Y., Silvestrini, B., Lee, W. M. and Cheng, C. Y. (1998) J. Androl. **19**, 686–703
37 Owen, D. J., Wigge, P., Vallis, Y., Moore, J. D. A., Evans, P. R. and McMahon, H. T. (1998) EMBO **17**, 5273–5285
38 Pawson, T. (1995) Nature (London) **373**, 573–580
39 Nakata, T., Iwamoto, A., Noda, Y., Takemura, R., Yoshikura, H. and Hirokawa, N. (1991) Neuron **7**, 461–469
40 Kudo, M., Saito, S., Sakagami, H., Suzaki, H. and Kondo, H (1999) Mol. Brain Res. **64**, 179–185
41 Nakata, T., Takemura, R. and Hirokawa, N. (1993) J. Cell Sci. **105**, 1–5
42 Woodhams, P. L., Webb, M., Atkinson, D. J. and Seeley, P. J. (1989) J. Neurosci. **9**, 2170–2181
43 Schmitt, I., Bachner, D., Megow, D., Henklein, P., Hameister, H., Epplen, J. T. and Riess, O. (1995) Hum. Mol. Genet. **4**, 1173–1182
44 Bhide, P. G., Day, M., Sapp, E., Schwarz, C., Sheth, A., Kim, J., Young, A. B., Penney, J., Golden, J., Aronin, N. and DiFiglia, M. (1996) J. Neurosci. **16**, 5523–5535
45 Strong, T. V., Tagle, D. A., Valdes, J. M., Elmer, L. W., Boehm, K., Swaroop, M., Kaatz, K. W., Collins, F. S. and Albin, R. L. (1993) Nat. Genet. **5**, 259–265
46 Li, S. H., Schilling, G., Young, III, W. S., Li, X. J., Margolis, R. L., Stine, O. C., Wagster, M. V., Abbott, M. H., Franz, M. L., Ranen, N. G. et al. (1993) Neuron **11**, 985–993
47 Hoogeveen, A. T., Willemsen, R., Meyer, N., Rooij, K. E., Roos, R. A. C., Ommen, G. J. B. and Galjaard, H. (1993) Hum Mol. Genet. **2**, 2069–2073
48 Hussain, N. K., Yamabhai, M., Ramjaun, A. R., Guy, A. M., Baranes, D., O'Bryan, J. P., Der, C. J., Kay, B. K. and McPherson, P. S. (1999) J. Biol. Chem. **274**, 15671–15677
49 Schmidt, A., Wolde, M., Thiele, C., Fest, W., Kratzin, H., Podtelejnikov, A. V., Witke, W., Huttner, W. B. and Soling, H. D. (1999) Nature (London) **401**, 133–141
50 Scales, S. J. and Scheller, R. H. (1999) Nature (London) **401**, 123–124
51 Cestra, G., Castagnoli, L., Dente, L., Minenkova, O., Petrelli, A., Migone, N., Hoffmuller, U., Schneider-Mergener, J. and Cesareni, G. (1999) J. Biol. Chem. **45**, 32001–32007
52 So, C. W., So, C. K. C., Cheung, N., Chew, S. L., Sham, M. H. and Chan, L. C. (2000) Leukemia **14**, 594–601
53 Micheva, K. D., Kay, B. K. and McPherson, P. S. (1997) J. Biol. Chem. **272**, 27239–27245

Received 26 October 1999/31 January 2000; accepted 8 March 2000